



First principles study of structural, electronic and magnetic properties of ferromagnetic $\text{Bi}_2\text{Fe}_4\text{O}_9$



Zainab Irshad^a, S.H. Shah^{a,b,c,*}, M.A. Rafiq^a, M.M. Hasan^a

^a Pakistan Institute of Engineering and Applied Sciences (PIEAS), P.O. Nilore, Islamabad 45650, Pakistan

^b Theoretical Physics Division, PINSTECH, Nilore, Islamabad, Pakistan

^c National Centre for Physics (NCP), Quaid-i-Azam University, Islamabad, Pakistan

ARTICLE INFO

Article history:

Received 5 September 2014

Received in revised form 20 October 2014

Accepted 31 October 2014

Available online 8 November 2014

Keywords:

$\text{Bi}_2\text{Fe}_4\text{O}_9$

Ferromagnetism

Electronic properties

Exchange interaction

Crystal field theory

Density functional theory

ABSTRACT

The structural, electronic, and magnetic properties of ferromagnetic bismuth ferrate ($\text{Bi}_2\text{Fe}_4\text{O}_9$) are investigated using density functional theory (DFT). Different exchange–correlation (xc) functionals (LSDA, PBE-GGA, PBEsol-GGA and WC-GGA) are tested to calculate various properties of $\text{Bi}_2\text{Fe}_4\text{O}_9$. All the exchange correlation functionals accurately describe the structural properties of $\text{Bi}_2\text{Fe}_4\text{O}_9$ but fail to calculate its correct band structure. The calculated band structure improves when DFT + *U* method is employed. The PBE-GGA + *U* calculations predict a bandgap of 2.1 eV for the ferromagnetic $\text{Bi}_2\text{Fe}_4\text{O}_9$ in close agreement with the experiment. The calculated density of states shows appreciable hybridization between Fe-3*d* states and O-2*p* states along with minor overlap between Bi-6*p* and O-2*p* states. The magnetic properties of $\text{Bi}_2\text{Fe}_4\text{O}_9$ are primarily due to Fe^{3+} ions, each of which has a non-integer magnetic moment of approximately 3.9 μ_B . The values of the induced magnetic moments at the other atomic sites depend on their local environments.

© 2014 Elsevier B.V. All rights reserved.

1. Introduction

The mullite type $\text{Bi}_2\text{Fe}_4\text{O}_9$ is attracting extensive research interest due to its interesting multiferroic [1], magnetic [2,3] and catalytic [4,5] properties. It is anticipated to have a wide range of applications as solid oxide fuel cells [6], semiconductor gas sensors [7], and spintronic devices [3]. $\text{Bi}_2\text{Fe}_4\text{O}_9$ is generally obtained as a by-product during the synthesis of BiFeO_3 [8–10]. The ferroelectric properties of this material stem from the stereochemical activity of Bi-6*s* lone electron pair whereas the magnetic behavior is due to the partially filled *d*-orbitals of Fe^{3+} ions [1]. Like BiFeO_3 [11,12], the physics of $\text{Bi}_2\text{Fe}_4\text{O}_9$ is rich [4,5,13,14]. A fundamental understanding of this material is, therefore, critical to realize its potential future applications. In the present study we provide atomic level insight into the structural, electronic and magnetic properties of ferromagnetic $\text{Bi}_2\text{Fe}_4\text{O}_9$.

$\text{Bi}_2\text{Fe}_4\text{O}_9$ belongs to the family of sillimanite and mullite type crystal structure [15]. The crystal system of $\text{Bi}_2\text{Fe}_4\text{O}_9$ is orthorhombic with space group *Pbam* (No. 55) [16,17]. Its unit cell consists of two formula units as shown in Fig. 1. The whole structure is characterized by the edge-sharing FeO_6 octahedra extended along

the *c*-axis which are connected by the corner-sharing FeO_4 tetrahedra [18]. The Fe atoms in the octahedral and tetrahedral environments are labeled as Fe(1) and Fe(2) respectively. There are four types of oxygen atoms labeled as O(1), O(2), O(3) and O(4). In each octahedron a Fe(1) atom is surrounded by O(1), O(2) and O(3) atoms whereas in each tetrahedron a Fe(2) atom is bonded with O(2), O(3) and O(4) atoms. The Bi atoms form highly distorted polyhedra which connect the octahedral chains.

The low temperature structure of $\text{Bi}_2\text{Fe}_4\text{O}_9$ is antiferromagnetic with a Neel temperature in the range of 237–265 K [1,3,19,20]. The magnetic moments of two types of Fe atoms could be arranged in a Cairo pentagonal lattice thus show a geometric frustration [21]. Interestingly it has been observed by Zhang et al. [5] that the small nanocrystals (<57 nm) of $\text{Bi}_2\text{Fe}_4\text{O}_9$ exhibit weak ferromagnetism. The origin of this weak ferromagnetism is the uncompensated surface spins of Fe^{3+} ions. In fact, weak surface ferromagnetism is a universal feature of nano-sized antiferromagnetic materials as proposed by Dzyloshinskii [22]. Similar effect of grain size on magnetism was also reported in nano-sized BiFeO_3 [9,23,24], $\text{La}_{1/3}\text{Sr}_{2/3}\text{FeO}_3$ [25], $\alpha\text{-Fe}_2\text{O}_3$ and La_2CuO_4 [26]. These experimental findings motivated us to investigate ferromagnetic properties of $\text{Bi}_2\text{Fe}_4\text{O}_9$.

Most of the research on $\text{Bi}_2\text{Fe}_4\text{O}_9$ is experimental with only a few theoretical studies. Iliev et al. [19] performed a combined experimental and computational study to investigate the phonon

* Corresponding author at: Theoretical Physics Division, PINSTECH, Nilore, Islamabad, Pakistan.

E-mail address: shafqatshah@gmail.com (S.H. Shah).

structure of $\text{Bi}_2\text{Fe}_4\text{O}_9$. Pchelkina and Streltsov [27] used DFT to study the microscopic origin of different exchange interactions in antiferromagnetic $\text{Bi}_2\text{Fe}_4\text{O}_9$. Previous experimental and theoretical studies have dealt with only antiferromagnetic phase of $\text{Bi}_2\text{Fe}_4\text{O}_9$. Computational studies of ferromagnetic $\text{Bi}_2\text{Fe}_4\text{O}_9$ have been overlooked.

In this paper, for the first time, we used full potential (linearized) augmented plane wave (FP-(L)APW) and local orbitals (lo) method, namely FP-(L)APW + lo method, based on density functional theory (DFT) to investigate the structural, electronic and magnetic properties of ferromagnetic phase of $\text{Bi}_2\text{Fe}_4\text{O}_9$. Different exchange correlation (xc) functionals such as LSDA [28], PBE-GGA [29], PBEsol-GGA [30] and WC-GGA [31] are tested to assess their applicability for bulk $\text{Bi}_2\text{Fe}_4\text{O}_9$. We argue that standard DFT functionals fail to calculate the correct electronic structure of $\text{Bi}_2\text{Fe}_4\text{O}_9$, therefore, it is vital to use DFT + U method based on Hubbard model [32]. In Section 2 we give computational details. Section 3 discusses the main results which include the structural, electronic and magnetic properties of ferromagnetic $\text{Bi}_2\text{Fe}_4\text{O}_9$. Section 4, summarizes the important results.

2. Computational details

We used one of the most accurate schemes of electronic structure calculations i.e., full potential (linearized) augmented plane wave (FP-(L)APW) and local orbitals (lo) method (FP-(L)APW + lo) as implemented in WIEN2k code [33]. It is a full potential method as it does not make any shape approximations for charge density and potential expansion. Different local (LSDA [28]) and semi local (PBE-GGA [29], PBEsol-GGA [30] and WC-GGA [31]) exchange correlation (xc) functional are used to calculate the structural and electronic properties of $\text{Bi}_2\text{Fe}_4\text{O}_9$. The muffin tin radii for Bi, Fe and O atoms are chosen as 2.02, 1.68 and 1.44 a.u. respectively. The basis set size for the wave functions is determined by $R_{\text{MT}}K_{\text{MAX}}$ which is set to be 7.0. Reciprocal space integration is performed with a $6 \times 5 \times 8$ mesh which represents 36 k -points in the irreducible Brillouin zone (IBZ). In order to simulate a ferromagnetic phase of $\text{Bi}_2\text{Fe}_4\text{O}_9$ the spins of all Fe^{3+} ions are aligned parallel.

First of all we calculated the equilibrium geometry of $\text{Bi}_2\text{Fe}_4\text{O}_9$ using different xc functionals. The geometry optimization is performed in two steps; first we calculated the equilibrium volume by optimizing b/a ratio with fixed volume and c/a ratio. Second,

once the volume of the system is optimized, the atomic positions are relaxed using a highly efficient algorithm based on simultaneous fixed-point optimization of density and atomic positions [34]. Self-consistency is achieved when the change in total energy, total charge density and calculated forces on all atoms is less than 1×10^{-4} mRy per unit cell, 1×10^{-3} e and 0.5 mRy/a.u. respectively. In the fully optimized $\text{Bi}_2\text{Fe}_4\text{O}_9$ system, total force on each atom is less than 2 mRy/a.u. All the subsequent calculations are performed using this optimized $\text{Bi}_2\text{Fe}_4\text{O}_9$ structure.

It is well known that systems containing 3d and 4f electrons such as transition metal oxides, rare earth metals and their compounds exhibit strong electronic correlation effect. Standard DFT exchange correlation functionals, being approximate in nature, fail to describe the correct electronic structure of such systems. Different remedies are proposed such as DFT + U [32], hybrid functionals [35], self-interaction correction methods [36], dynamical mean field theory (DMFT) [37] and highly accurate quantum Monte Carlo method [38]. Among all these techniques DFT + U method is reasonably accurate, well tested and computationally less intensive. Three different variants of DFT + U method are implemented in WIEN2k; among which we selected the one introduced by Anisimov et al. [39]. They defined an approximate correction to electronic self-interaction using $U_{\text{eff}} = U - J$ where U and J are on-site Coulomb and exchange parameters respectively. We have calculated U_{eff} for $\text{Bi}_2\text{Fe}_4\text{O}_9$ following the procedure adopted by Anisimov et al. [32,40]. Our calculated U_{eff} for Fe^{3+} ions is 4.5 eV (where $U = 4.5$ eV and $J = 0$) which is close to U_{eff} used in different studies [27]. We used $U_{\text{eff}} = 4.5$ eV to calculate the electronic and magnetic properties of $\text{Bi}_2\text{Fe}_4\text{O}_9$.

3. Results and discussion

In order to determine the equilibrium structure of $\text{Bi}_2\text{Fe}_4\text{O}_9$, geometry optimization of the experimental structure is performed using different xc functionals. First volume of the system is optimized and then atomic positions are completely relaxed. Tables 1 and 2 give the optimized lattice parameters and atomic positions respectively. It is noteworthy that all the xc functionals describe $\text{Bi}_2\text{Fe}_4\text{O}_9$ structure very well. The spin polarized LDA (LSDA [28]) gives the most accurate lattice parameters (maximum 0.5% deviation) whereas WC-GGA [31] gives the least accurate values (maximum 1.03% deviation) of the calculated lattice parameters compared to the corresponding experimental values. All the xc functionals overestimate the b lattice parameter and the b/a ratio whereas underestimate the a and c lattice parameters. It is important to note here that the lattice parameters of $\text{Bi}_2\text{Fe}_4\text{O}_9$ exhibit anisotropic behavior under high pressure (0–34 GPa) [16] and temperature (0–1173 K) [41]. For instance, under high pressure (0–26 GPa) [16], the lattice parameter c is least compressible whereas the a lattice parameter is the most compressible. The compressibility of the b lattice parameter is higher than the c lattice parameter at low pressure range (<7 GPa) and less than the c at high pressure range (>7 GPa). Similarly, at high temperature the thermal expansion coefficient of the b lattice parameter is larger than those of the a and c lattice parameters [41]. All the xc functionals used in this study accurately calculate all the atomic positions. The maximum deviation from the experimental value is less than 0.02% as shown in Fig. 2. The atomic position of O(4) atom shows no deviation from the experimental value as it is constrained at a high symmetry position (i.e., Wyckoff position 2b). Under high pressure (≈ 6 GPa), O(4) atom moves to a less symmetrical position (i.e., Wyckoff position 4c) indicating the onset of a high pressure phase transition in $\text{Bi}_2\text{Fe}_4\text{O}_9$ [16]. The calculated bond lengths and bond angles are also in excellent agreement with the experimental data, as given by Table 2. The behavior of different xc functionals for bond lengths and bond angles is random. The maximum deviation

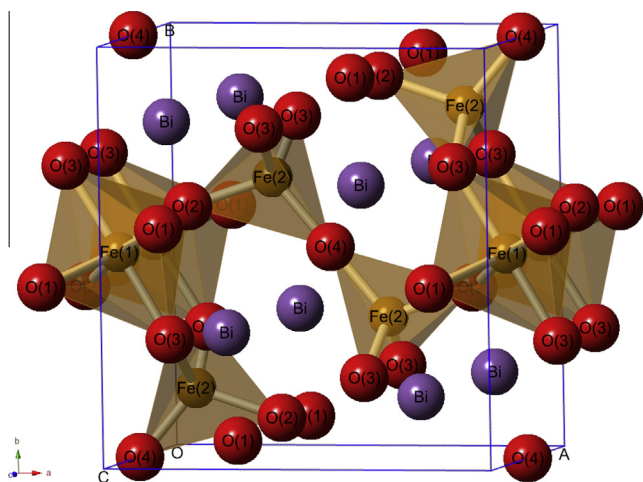


Fig. 1. Crystal structure of $\text{Bi}_2\text{Fe}_4\text{O}_9$. The Bismuth (Bi), iron (Fe(1) and Fe(2)) and oxygen (O(1), O(2), O(3) and O(4)) atoms are represented by purple, brown and red colored balls. All the Fe(1) and Fe(2) atoms are in octahedral and tetrahedral environments respectively. (For interpretation of the references to color in this figure legend, the reader is referred to the web version of this article.)

Download English Version:

<https://daneshyari.com/en/article/1609801>

Download Persian Version:

<https://daneshyari.com/article/1609801>

[Daneshyari.com](https://daneshyari.com)